Spectrochimica Acta Part A: Molecular and Biomolecular Spectroscopy 199 (2018) 349–355

Contents lists available at ScienceDirect

Spectrochimica Acta Part A: Molecular and Biomolecular Spectroscopy

journal homepage: www.elsevier.com/locate/saa

Geometry-dependent DNA-TiO_2 immobilization mechanism: A spectroscopic approach

M.O. Silva-Moraes [a], Y. Garcia-Basabe [b], R.F.B. de Souza [a], A.J. Mota [c], R.R. Passos [a], D. Galante [d], H.D. Fonseca Filho [e], Y. Romaguera-Barcelay [e], M.L.M. Rocco [f], W.R. Brito [a,*]

[a] Department of Chemistry, Federal University of Amazonas, Manaus, Amazonas 69067-005, Brazil
[b] Institute of Science of Life and Nature - ILACVN, Federal University of Latin-American Integration, Foz do Iguaçu 85866-000, PR, Brazil
[c] Faculty of Agricultural Sciences, Federal University of Amazonas, Manaus, Amazonas 69067-005, Brazil
[d] Brazilian Synchrotron Light Laboratory LNLS/CNPEM, Campinas, São Paulo 13083-970, Brazil
[e] Department of Physics, Federal University of Amazonas, Manaus, Amazonas 69067-005, Brazil
[f] Institute of Chemistry, Federal University of Rio de Janeiro, Rio de Janeiro, Rio de Janeiro 21941-901, Brazil

ARTICLE INFO

Article history:
Received 30 October 2017
Received in revised form 28 March 2018
Accepted 30 March 2018
Available online 03 April 2018

Keywords:
Electrochemical sensor
DNA-based biosensor
Charge transfer
DNA immobilization
X-ray photoelectron spectroscopy
X-ray absorption spectroscopy

ABSTRACT

DNA nucleotides are used as a molecular recognition system on electrodes modified to be applied in the detection of various diseases, but immobilization mechanisms, as well as, charge transfers are not satisfactorily described in the literature. An electrochemical and spectroscopic study was carried out to characterize the molecular groups involved in the direct immobilization of DNA structures on the surface of nanostructured TiO_2 with the aim of evaluating the influence of the geometrical aspects. X-ray photoelectron spectroscopy at O1s and P2p core levels indicate that immobilization of DNA samples occurs through covalent (P—O—Ti) bonds. X-ray absorption spectra at the Ti2p edge reinforce this conclusion. A new species at 138.5 eV was reported from P2p XPS spectra analysis which plays an important role in DNA-TiO_2 immobilization. The P—O—Ti/O—Ti ratio showed that quantitatively the DNA immobilization mechanism is dependent on their geometry, becoming more efficient for plasmid ds-DNA structures than for PCR ds-DNA structures. The analysis of photoabsorption spectra at C1s edge revealed that the molecular groups that participate in the C1s → LUMO electronic transitions have different pathways in the charge transfer processes at the DNA-TiO_2 interface. Our results may contribute to additional studies of immobilization mechanisms understanding the influence of the geometry of different DNA molecules on nanostructured semiconductor and possible impact to the charge transfer processes with application in biosensors or aptamers.

1. Introduction

DNA nucleotides are used as molecular recognition system, double stranded deoxyribonucleic acid (ds-DNA) is a well characterized system, a double helix formed when two single strands are paired by hydrogen bonds to form a long chain of nitrogenous base pairs, Adenine-Thymine and Cytosine-Guanine (A-T and C-G). A single strand DNA (ss-DNA) is formed by a polyanionic sugar-phosphate backbone connected to the nitrogenous bases, rich in π-bonds. This is a system that contains a stack of π-orbitals extending within the DNA, facilitating electron transfer, which is one of the reasons for the various applications of DNA structure in biosensors devices [1,2].

DNA-based biosensors consist of the immobilized DNA strand to detect the complementary nucleic acid sequence by DNA target hybridization. DNA immobilization on the surface of electrodes can be applied in the detection of viral diseases [3–5]. These detection devices depend on the efficiency of charge-transfer processes (electric signal) occurring from the complementary and/or adjacent nucleobases of the tris-phosphate groups to the conductor or semiconductor substrate. Understanding the characteristics of the immobilization of different geometrical structures of DNA it is possible to deepen into the charge transfer mechanisms relevant for application in DNA-based biosensors. The interaction of biomolecule and the substrate surface involve covalent, ionic, hydrogen or van der Waals bonding that depends on the molecular structure, size and the nanostructured metal oxide properties (i.e. surface charges, energy, functional groups, etc.) [6,7].

TiO_2 is widely used as a semiconductor material functionalized with molecules due to its high biocompatibility, high stability, easy availability and low cost [8,9]. Connor et al. have demonstrated that the phosphate groups perform electrostatic interactions with TiO_2 using internal reflectance spectroscopy (IRS) [10], and Liu et al. studied the photo-oxidation of ds-DNA immobilized on TiO_2 films by cyclic voltammetry [11].

* Corresponding author.
E-mail address: wrbrito@ufam.edu.br. (W.R. Brito).

https://doi.org/10.1016/j.saa.2018.03.081
1386-1425/

This work aims to study chemical species involved in the mechanisms of direct immobilization of the *Escherichia coli* plasmid ds-DNA (pDNA) and PCR ds-DNA (PCR) on TiO_2. For this purpose, a combination of electrochemical and core-level spectroscopic characterizations was performed. Our results showed that these DNA molecules are immobilized on TiO_2 surface through P—O—Ti bonds, and that immobilization efficiency depends on the DNA geometry. The charge transfer process between DNA molecules and TiO_2 substrate were elucidated by cyclic voltammetry and corroborated by C K-edge and Ti L-edge X-ray absorption.

2. Experimental

2.1. Materials and Methods

Titanium (IV) isopropoxide (97%), ethanol (99.5%) and hydrochloric acid (37%) were purchased from Sigma-Aldrich. ITO (Indium Tin Oxide) coated on glass (75 × 50 × 0.7 mm, surface resistivity 15 Ω/sq) was obtained from (Lumtech, Taiwan). Tris hydrochloride (Tris-HCl) solution, Ethylenedinitrilotetraacetic acid (EDTA) buffer, Tris-EDTA buffer solution, glucose solution, sodium hydroxide P.A., sodium dodecyl sulfate solution, sodium hypochlorite solution, potassium acetate, glacial acetic acid, chloroform, and isopropanol were purchased from Sigma-Aldrich. dNTP Set was acquired from Thermo Scientific and Platinum Taq DNA Polymerase were acquired from Invitrogen™.

2.2. dsDNA Samples (gDNA, pDNA and Amplicon)

The pCR™ 2.1-TOPO® (Invitrogen by Thermo) plasmid vector (pDNA) extraction was performed through the alkaline lysis method [12]. The 200 bp amplicon was obtained copying a known fragment of pDNA though the Polymerase Chain Reaction (PCR) method using the Taq DNA Polymerase Platinum kit (Invitrogen™ by Thermo Scientific) and M13 primers, following the manufacturer's recommendations. The sequence of nitrogenous bases from a plasmid strand and PCR-DNA are found in Supplementary material of this paper.

2.3. TiO_2 Films and Synthesis

The nanostructured TiO_2 was synthesized through the sol-gel method according to the literature [13]. A container containing 2.3 mL of Titanium (IV) isopropoxide, 7.6 mL of ethanol and 15.0 mL of hydrochloric acid was stirred for 6 h. The TiO_2 films were produced by adding an aliquot of the sol-gel of TiO_2 over ITO (Indium Tin Oxide)/glass substrates (15 × 15 mm) using the spin coating method at 3000 rpm by 60 s. Subsequently, the TiO_2/ITO films were sintered in a muffle at 350 °C for 45 min.

The surface morphology of the TiO_2/ITO film was obtained with an AFM (Innova, Bruker) on an area of (20 × 20) μm^2, operated in contact mode using silicon nitride cantilevers to scan the samples. They were performed with 512 × 512 pixels at a scan rate of 1.0 Hz. All measurements were performed at room temperature (296 ± 1 K) and 40 ± 1% relative humidity. The feedback control was adapted to the surface in order to obtain the best possible images, and they were analysed using the WSxM software [14] for determining the films surface roughness and thickness, as shown in in Fig. SI1 in Supplementary material. The films AFM images show a surface roughness of 1.02 nm and thickness of 15 nm, representative of a homogeneous surface.

2.4. DNA Immobilization

According to Scheme 1, the TiO_2/ITO films were immersed in two container containing 2.0 mL of deionized water, one with pDNA pellet, and another, with PCR pellet overnight at 4 °C for DNA immobilization. The DNA solutions were kept in phosphate buffer of pH 4. Afterwards, the films were vigorously washed with deionized water to remove the excess of DNA or DNA samples that have done weak bonds on the TiO_2 film surface, and dried at room temperature. The films were taken to an oven for 30 min at a temperature of 70 °C. The investigated samples will be labelled here as TiO_2/ITO, pDNA/TiO_2/ITO and PCR/TiO_2/ITO for nanostructured TiO_2 and immobilized DNA-TiO_2 films, respectively.

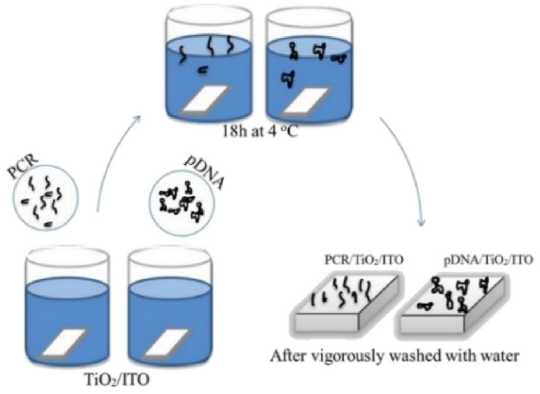

Scheme 1. DNA immobilization procedure on TiO_2/ITO surfaces in aqueous solution.

2.5. Electrochemical Experiments

The DNA immobilization was characterized by cyclic voltammetry (CV) in a conventional three-electrode configuration using the AUTOLAB PGSTAT 302N potentiostat (Metrohn Autolab, Utrecht, The Netherlands) equipped with GPES 4.9 software. The reference electrode was Ag/AgCl (3 M KCl) and the auxiliary electrode was a platinum wound wire. The working electrodes used in the experiment contained a total area of 15 × 10 mm ITO/glass, and the samples of interest were deposited at 10 × 10 mm. In the CV assays, a solution of methylene blue of 2.0 $\mu mol \cdot L^{-1}$ was used as electrolyte and intercalator at a scanning rate of 50 mV/s.

2.6. NEXAFS Experiments

Near edge X-ray absorption fine structure (NEXAFS) experiments were performed at the SGM beamline (250–1000 eV) at the Brazilian Synchrotron Light Source (LNLS), in Campinas, Brazil. Samples of TiO_2/ITO, pDNA/TiO_2/ITO and PCR/TiO_2/ITO were fixed on the sample holder with a carbon conductive tape and introduced into the ultra-high vacuum chamber (10^{-8} mbar). NEXAFS spectra were obtained in the total electron yield (TEY) mode at carbon, K absorption edge and titanium L-edge, before and after pDNA and PCR-DNA immobilization on nanostructured TiO_2. The spectra were normalized by the incident photon flux (I_0) measured with an Au mesh placed just upstream of the sample. Phenylalanine was used as standard reference for photon energy calibration of the NEXAFS spectra [15]. NEXAFS spectra shown in this work were background corrected by a linear pre-edge subtraction and linear regression beyond the edge.

2.7. XPS Experiments

X-ray photoelectron spectroscopy (XPS) measurements were performed at the ESCALAB 250Xi spectrometer (Thermo Scientific) equipped with an electron energy hemispherical analyzer using monochromatized Al Kα line ($h\upsilon = 1486.6$ eV) excitation. The spectra were energy referenced to the C1s signal of aliphatic C atoms at binding energy of 285.00 eV. XPS spectra were collected using X-ray beam spot size = 650 μm and with emission angle of 0° with respect to the sample surface. Survey spectra were measured from 0 to 1300 eV with pass energy of 50 eV and high resolution spectra acquired with 25 eV pass energy at C1s, N1s, O1s, Ti2p and P2p core levels. Sensitivity factors were

used to determine the atomic concentrations of each element in the samples [16]. The spectra were collected at two different points of the sample surface for evaluated the chemical homogeneity of the films.

3. Results and Discussion

The electrochemical behavior of pDNA/TiO_2/ITO, PCR/TiO_2/ITO and TiO_2/ITO electrodes was studied using as electrolyte and intercalator a methylene blue solution. Fig. 1 shows comparative cyclic voltamogramns in which it is possible to observe two significant differences: i) the anodic and cathodic peaks in the voltamogramns of pDNA/TiO_2/ITO and PCR/TiO_2/ITO electrodes show a shift in relation to TiO_2/ITO electrode that implied different electrochemical responses and electrode modification. This shift is probably due to the methylene blue interaction with the cytosine and guanine sequences, intercalating the π-stacking [17–19].

The reduction of methylene blue can occur by two mechanisms: first, through DNA-mediated charge transfer (intercalation); second, through the direct reduction on the surface of TiO_2 [18,19]. An attenuation of the current signal of the PCR curve was observed when compared to the curve of the immobilized pDNA. The passivation of the PCR/TiO_2/ITO film may be related to the charge transport properties intrinsic to the base sequence that constitutes the molecular structure of the PCR. ii) the bigger current density present in electrodes DNA functionalized than TiO_2/ITO, indicating a greater binding capacity to produces a reversible redox couple via-charge transfer with methylene blue, as a reported by Pheeney and Barton [19].

This electrochemical performance can be explained by the two different geometries of the immobilized DNA structures that influence the charge mobility mechanism through the work electrode, theses points are better exploited with spectroscopic techniques. In Fig. 2 (a) the XPS survey spectra for pDNA/TiO_2/ITO/glass, PCR/TiO_2/ITO/glass and TiO_2/ITO/glass films are presented. All characteristic peaks for TiO_2, ITO and DNA samples, as C1s, O1s, Ti2p, In3d and Sn3d core levels were identified. The presence of In3d, Sn3d and Ti2p core levels in the XPS survey spectra is evidence that TiO_2 ultrathin films were deposited onto ITO substrate and confirmed by AFM image analysis (see Fig. SI1 in Supplementary material). On the other hand, the presence of C1s core level at pDNA/TiO_2/ITO/glass and PCR/TiO_2/ITO/glass XPS spectra is an indication that DNA molecules are adsorbed on the TiO_2 surface. N1s and P2p peaks were not directly observed in the survey spectra of DNA samples, probably due to the low photoionization cross-sections for these core levels using Al Kα photon energy and also to the low concentration (very thin films) of DNA on the TiO_2 films. Then, the high-resolution N1s and P2p XPS spectra for pDNA and PCR samples were measured and are presented in Fig. 2(b) and (c), respectively.

The deconvolution of these spectra allowed us to carry out the assignments for the different chemical environments of nitrogen and phosphorus atoms. The high-resolution N1s spectra of the DNA-TiO_2 samples were deconvoluted using three contributions centred at 398.5, 399.8 and 401.5 eV for PCR and 398.1, 399.8 and 401.3 eV for pDNA, respectively. These contributions can be attributed to the imine (—N═), amine (—NH—) and amino ($—NH_2$) nitrogen species, respectively [20–24].

No significant changes are observed at the N1s spectra for both DNA samples analysed here and their profile are indeed very similar to DNA samples, which suggests lower participation of nitrogen species in DNA-TiO_2 immobilization. On the other hand, high resolution P2p spectra are characterized by two contributions: the first one appears at 133.4 eV, is labelled as 1 in Fig. 2(c) and assigned to phosphate backbone (PO_4) present in the DNA structure [21–24]; the other contribution, labelled as 2 in Fig. 2(c), appears at 138.5 eV and has never been reported before in DNA immobilization on semiconductor and conductor surfaces. The last contribution may be due to the interaction between DNA phosphate groups and the TiO_2 surface. Phosphorus species whit binding energy close to 138.5 eV has been only reported by Yan et al. on gas phase volatile phosphorus compounds containing polarizable ligands [25]. However, recently, Taucher et al. showed that electrostatic effects can influence significantly the measured core-level binding energies [26]. Then, this P2p contribution at high binding energy could be influenced by electrostatic interaction between DNA and TiO_2.

The spin-orbit doublet $2p_{3/2}$ and $2p_{1/2}$ components with energy separation of 0.85 eV are clearly identified in both P2p spectra. A notable reduction of the phosphate group contribution due to covalent DNA-TiO_2 is clearly observed for pDNA/TiO_2/ITO sample. The new species at 138.5 eV labelled as 2 plays an important role in pDNA-TiO_2 immobilization. The origin of this species will be discussed below. The quantitative chemical analysis obtained from XPS survey and high resolution N1s and P2p spectra for both DNA samples are reported in Table 1.

High-resolution O1s XPS spectra for TiO_2/ITO, PCR/TiO_2/ITO and pDNA/TiO_2/ITO are illustrated in Fig. 3. O1s spectrum of TiO_2/ITO substrate was deconvoluted into two contributions appearing at 530.0 eV and 531.3 eV and ascribed to O^{2-} of titanium oxide and to weakly physical adsorbed oxygen species such as OH groups on the surface (Ti-OH), respectively [22,27]. Three contributions were used in the deconvolution of the O1s DNA spectra. Besides the two oxygen observed in TiO_2/ITO

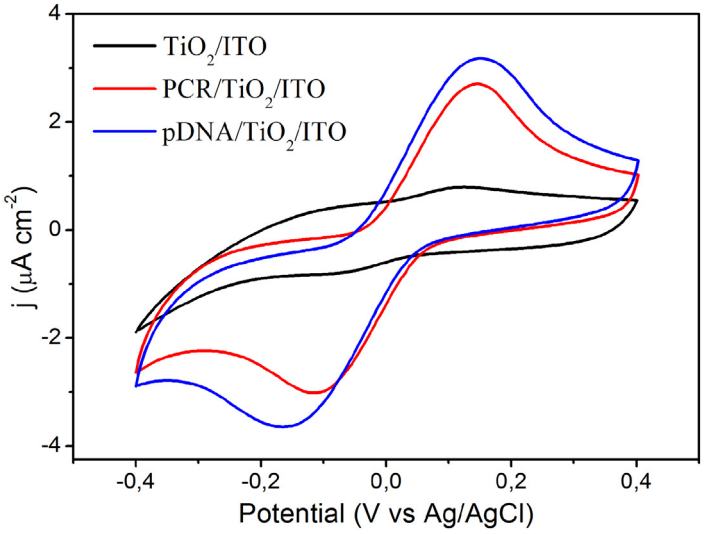

Fig. 1. Cyclic voltammogram of the TiO_2/ITO (black curve), PCR/TiO_2/ITO (red curve) and pDNA/TiO_2/ITO (blue curve) and in MB 2.0 μmol·L^{-1} solution. (For interpretation of the references to color in this figure legend, the reader is referred to the web version of this article.)

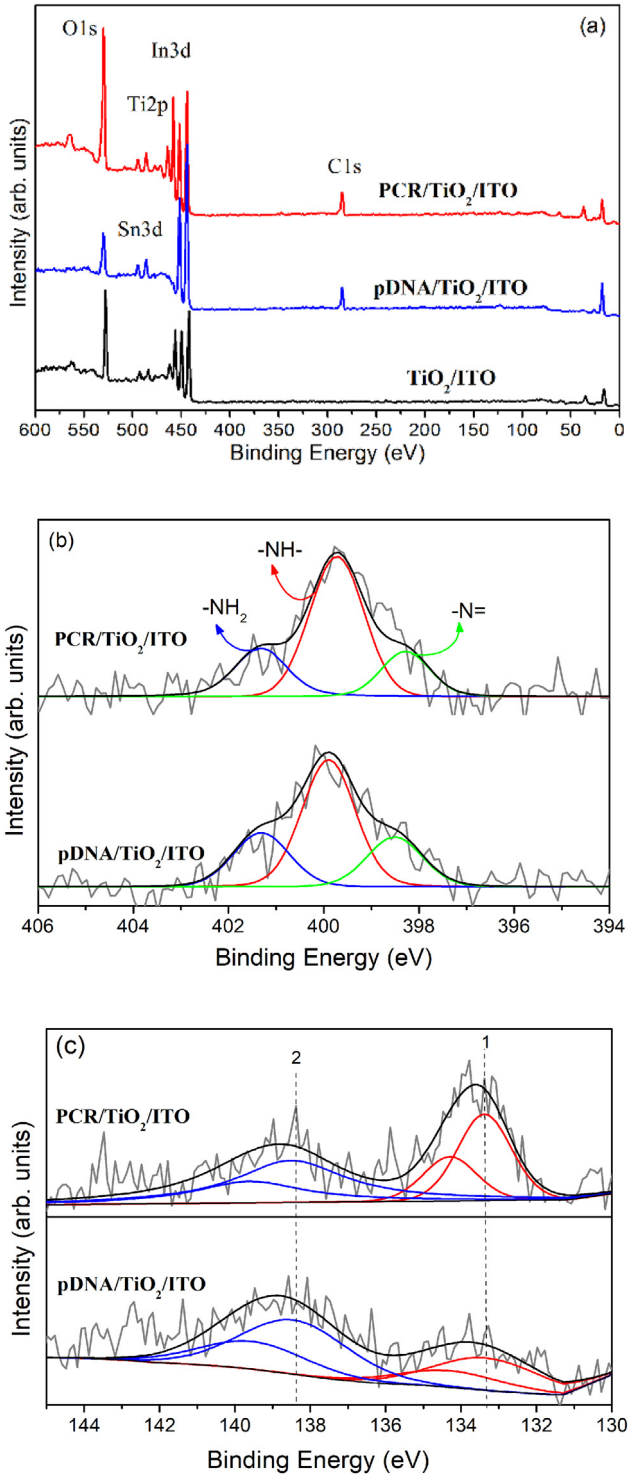

Fig. 2. XPS survey spectra of PCR/TiO_2/ITO, pDNA/TiO_2/ITO and TiO_2/ITO films (a). High-resolution N1s (b) and P2p (c) XPS spectra of PCR/TiO_2/ITO and pDNA/TiO_2/ITO.

Table 1
Elemental composition (at%) of pDNA/TiO_2/ITO and PCR/TiO_2/ITO films obtained from XPS spectra analysis. The P atomic % was divided into two components (1) and (2), corresponding to phosphate of the DNA backbone and P—O—Ti, respectively.

	Atomic percentage							
	C1s	O1s	N1s	P2p(1)	P2p(2)	Ti2p	In3d	Sn3d
PCR	22.7%	47.6%	0.9%	0.6%	0.8%	19.3%	7.0%	0.9%
pDNA	34.3%	32.2%	1.0%	0.2%	0.7%	18.9%	11.3%	1.4%

substrate, other oxygen species is found at binding energy of ≈532.7 eV in PCR and 532.6 eV in pDNA, respectively [28–30]. This species was attributed to O—C, O═C bonds in DNA molecules (nitrogenous bases and deoxyribose). The increase in component intensity at 531.2 eV was attributed to P—O—Ti bonding between the tris-phosphate group of the PCR and pDNA structure and TiO_2 surface [31,32]. However, according to quantitative analysis of the O1s, P2p and N1s core levels the most probable contribution in pDNA sample is P—O—Ti species.

Previous studies have shown that DNA immobilization on TiO_2 films occurs through tris-phosphate groups that, in aqueous solution, assume a negative charge density, while on TiO_2 surface they form positively charged layers [10,11]. Thus, on the DNA-TiO_2 interface in aqueous solution, the interactions are mainly of the electrostatic type. As already known, TiO_2 may present oxygen vacancies [33], and the negatively charged oxygen from the phosphate group can interact with empty 3d orbitals of titanium, forming covalent bonds producing a characteristic photoelectron peak at 531.2 eV binding energy [31,32] which could be evidenced by our XPS spectroscopy results. The fitting results are shown in Table 2. Peak areas were used to determine the atomic percentage of oxygen species in different chemical environments, specifically O—Ti, P—O—Ti, and O═C. The primary interest of this study is to determine the relative concentration of P—O—Ti/O—Ti species as an evidence of the DNA immobilization samples on the TiO_2 surface. The ratio between P—O—Ti/O—Ti oxygen species calculated from Table 2 was 0.17 and 0.24 for PCR/TiO_2/ITO and pDNA/TiO_2/ITO samples, respectively. A similar trend is observed for phosphorous species reported in Table 1, where the contribution labelled as 2 on P2p XPS spectra is higher than for pDNA/TiO_2 film.

This result allows us to associate this phosphorous species to P—O—Ti link. The combination of O1s and P2p results shows that the immobilization involving P—O—Ti species is more efficiently for pDNA/TiO_2/ITO sample. Some factors may be contributing to these quantitative results, as for example, the DNA molecule geometry and ordering. It is well known that plasmid DNA molecule presents a well-ordered structure compared to PCR. This together with circular geometry of the pDNA molecule can help to increase the contact area between the molecule and substrate [34]. Besides, PCR-DNA is a short and linear fragment with less contact area to anchoring to TiO_2 surface [35].

DNA immobilization on the TiO_2 films was also investigated by NEXAFS spectroscopy. This is a technique highly sensitive to chemical changes of material surfaces and, therefore, capable of determining the density of unoccupied electronic states in DNA/TiO_2 interface. Fig. 4 shows C K-edge NEXAFS spectra for the pDNA/TiO_2/ITO and PCR/TiO_2/ITO films. The main electronic transitions characterizing the C1s absorption spectra of DNA samples are C1s → π*C═C (285.4 eV), C1s → π*C═N (286.9 eV), C1s → π*HNC═O (287.6 eV), C1s → σ*C—C (294.0 eV) and a weak feature attributed to C1s → σ*C—O (297.0 eV) [36–38].

NEXAFS spectra on the C K-edge showed different intensities and profiles. In the PCR spectrum it was observed that C1s → π*C═N transitions are more intense than C1s → π*C═O transitions, whereas in the pDNA spectra the intensities of these transitions are nearly similar. These results suggest that the charge transfer processes follow different pathways within the analysed DNA-TiO_2 system. The C1s XPS measurements corroborate this observation. In the inset of Fig. 4(a) and (b), the deconvoluted C1s XPS spectra show that C—N and C—O peaks have similar behavior to that observed in the C K-edge NEXAFS spectra.

The literature [39,40] reports that the number of neighbouring guanines of G-G and G-G-G types in same tape favours charge transfer process through π orbitals with the purine ring stacked along the chain. The greater presence of neighbouring guanines, the greater is the probability that the DNA structure behaves as a conductive material. The plasmid DNA has 7858 nitrogenous bases with GG = 330 and GGG = 93 neighbours, whereas the PCR has 400 nitrogenous bases with GG = 20 and GGG = 3 (as showed in the Table SI1†). The ratio between the guanine bases shows qualitatively the conductive behavior of the DNA

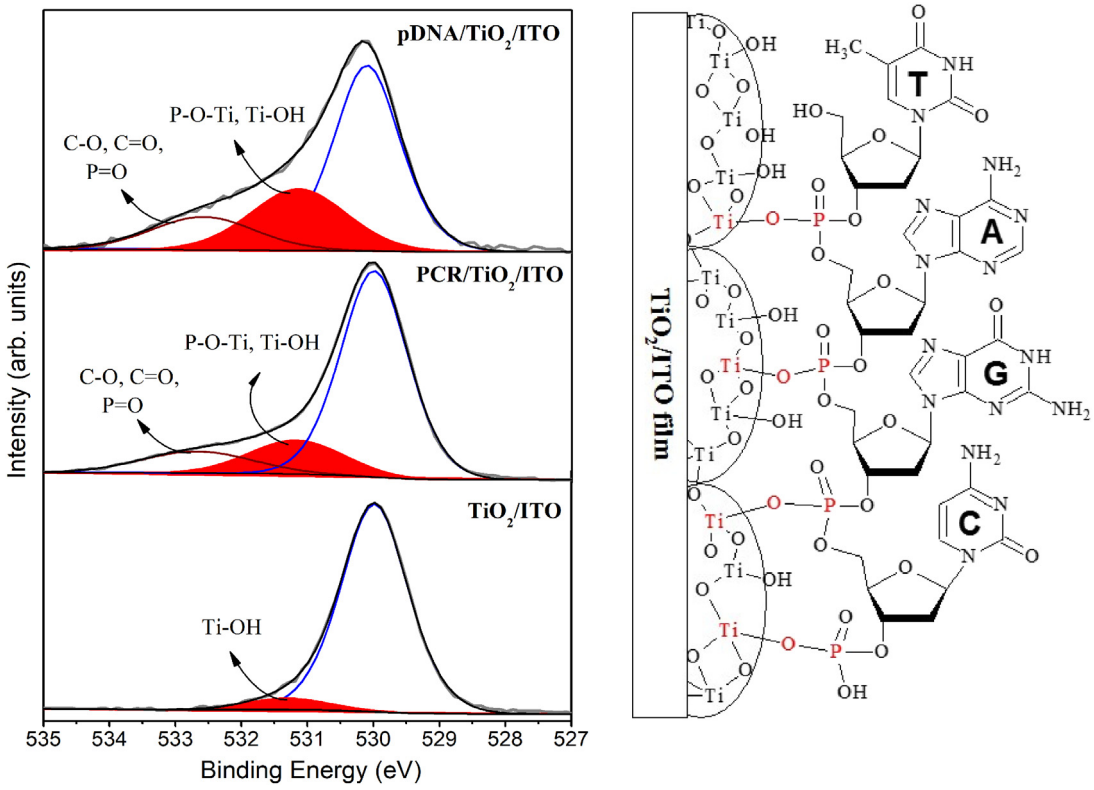

Fig. 3. Deconvolution of the O1s XPS spectra for pDNA/TiO_2/ITO, PCR/TiO_2/ITO, and TiO_2/ITO samples. In the inset, DNA immobilization on TiO_2/ITO through tri-phosphate groups.

samples. In this way, the GGG/GG ratio indicates that pDNA (0.28) is more conductive than PCR (0.15). Details are given of the complete plasmid DNA and PCR sequence is given in the Supplementary material. It was suggested in the literature [41] that the HOMO-LUMO gap of the ds-DNA is related to the phenomenon of charge drop with a band gap of 2.6 eV associated to a transition between the π and π* orbitals. The qualitative comparison between the intensities of the C K-edge NEXAFS spectra showed that the PCR has more empty states than the plasmid DNA. Thus, the PCR has greater probability of receiving electrons in the unoccupied orbitals and, therefore, has a higher reactivity. So, we conclude that the plasmid DNA compared to the PCR presents greater stability.

Fig. 5 shows the Ti L-edge NEXAFS spectra for the TiO_2, PCR/TiO_2/ITO and pDNA/TiO_2/ITO films. Ti L-edge NEXAFS spectrum is characterized by a set of peaks associated to L_3 (a_1 and a_2) resulting from $2p_{3/2}$ transition to $3d_{5/2}$ final state and L_2 (b_1 and b_2) resulting from $2p_{1/2}$ transition to $3d_{3/2}$ final state. The character of these states is modified by the combined spin-orbit and crystal field interactions. The peak splits (L_3 and L_2) correspond to transitions involving t_{2g} (a_1 and b_1) and e_g (a_2 and b_2) orbitals in an octahedral symmetry slightly distorted TiO_2 structure [39,40,42]; the same pattern was observed for the NEXAFS spectra of PCR/TiO_2/ITO and pDNA/TiO_2/ITO in terms of peak splitting and symmetry. Remembering that in X-ray absorption spectroscopy, the core electron is excited to empty electronic states, the transitions are observed only if these states are unoccupied.

Table 2
Binding energy (BE) values and atomic percentage (at%) of molecular groups for TiO_2/ITO substrate and DNA samples from high-resolution O1s XPS measurements.

Samples	TiO_2/ITO		PCR		pDNA	
	BE (eV)	at%	BE (eV)	at%	BE (eV)	at%
O—Ti	530.0	93.9	530.0	34.3	530.1	19.3
P—O—Ti/Ti—OH	531.3	6.13	531.2	7.6	531.2	8.2
C═O/P═O	–	–	532.7	5.7	532.6	4.7

The intensity of the peaks can be used to estimate the density of unoccupied states, qualitatively. Both PCR and pDNA are immobilized on TiO_2 thin film, and the transitions to unoccupied states for the L_3 (e_g) and L_2 (e_g) do not vary in intensity, but for the L_3 (t_{2g}) and L_2 (t_{2g}) there is a significantly change relative to TiO_2/ITO [43]. The electrons in t_{2g} electronic states are concentrated in the space between the incoming ligand in TiO_2 octahedral coordination, while e_g orbital points straight at the incoming ligands. The t_{2g} orbitals have the incorrect symmetry to participate in sigma interactions with the ligands. However, they have the correct symmetry to participate in π-interactions with the ligands. This indicates that there is chemical interaction between the DNA samples and the TiO_2 surface through Ti t_{2g} electronic states with a π-character [44–46]. The π-symmetry of the electronic states involved in DNA anchoring results in high electron mobility between molecule and substrate which is an important point for a successful application in biomaterials.

4. Conclusions

This study aimed to investigate different aspects related to the influence of the geometry of the different DNA structures immobilized on TiO_2 and approach to the charge transfer mechanisms. Electrochemical experiments showed that the DNA molecule was successfully immobilized on the semiconductor, being possible to emphasize that the pDNA has more intercalation effects than PCR with methylene blue, as well as that the presence of DNA molecules decreases the charge transfer resistance of the TiO_2 film. New phosphorous specie at 138.5 eV was reported from P2p XPS spectra analysis which plays an important role in DNA-TiO_2 immobilization. This specie is associated to P—O—Ti bond between phosphate backbone (PO_4) present in the DNA structure and TiO_2 substrate surface. From the quantitative analysis of the O1s XPS spectra, the P—O—Ti/O—Ti ratio showed that immobilization through the tris-phosphate groups was higher for the plasmid ds-DNA (0.24) than for the PCR ds-DNA (0.17).

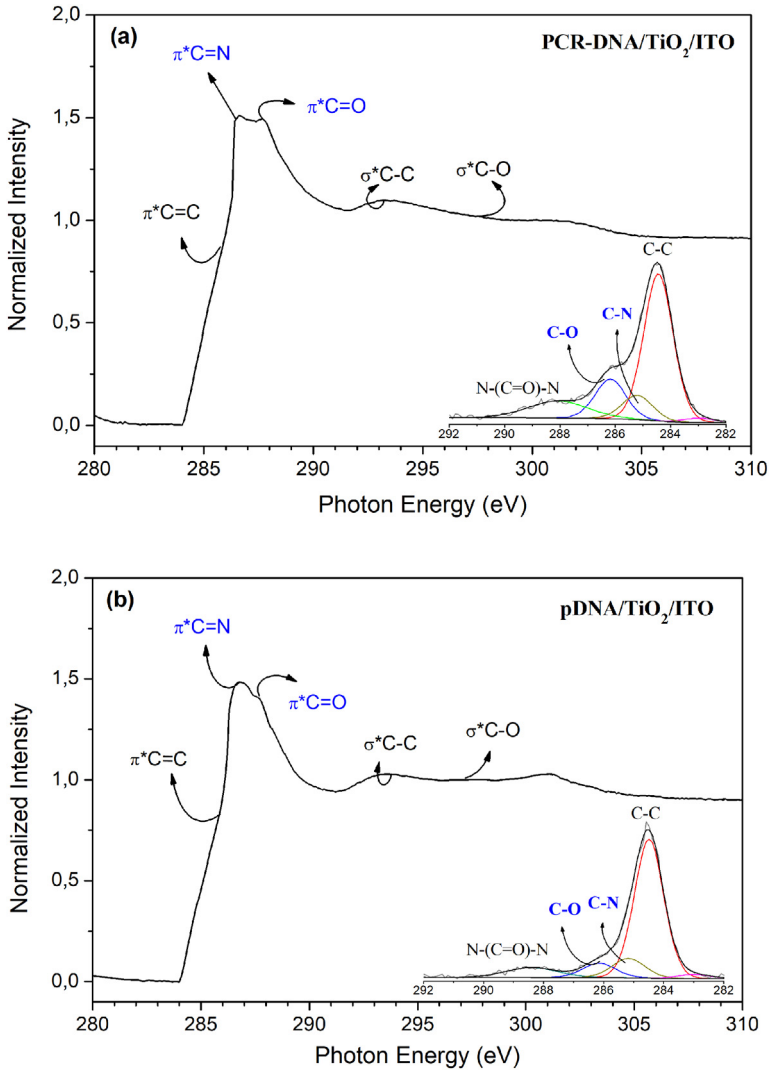

Fig. 4. C K-edge spectrum for PCR/TiO_2/ITO (a) and for pDNA/TiO_2/ITO (b). Inset, deconvolution of the C1s XPS spectra of PCR/TiO_2/ITO and pDNA/TiO_2/ITO samples.

The analysis of the C K-edge NEXAFS spectra showed that the charge transfer processes follow different pathways within the studied DNA/TiO_2 systems. The Ti L-edge NEXAFS spectra revealed that the immobilization of DNA occurs through empty Ti 3d orbitals and O 2p orbitals of oxygen atoms from tri-phosphate groups, involving mainly Ti t_{2g} electronic states with a π-character.

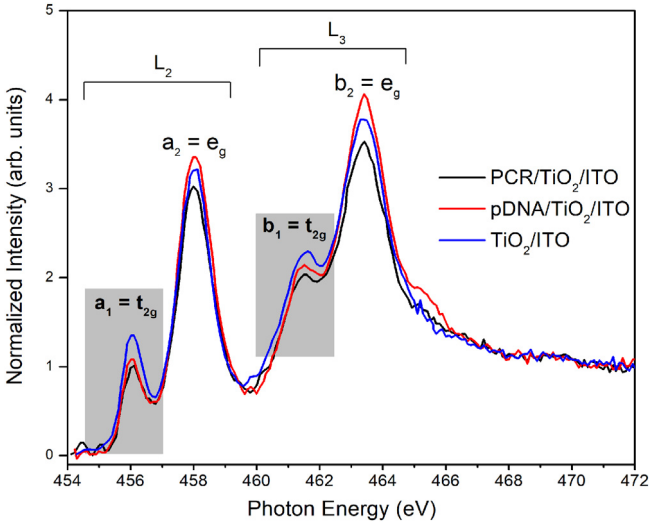

Fig. 5. Ti L-edge NEXAFS spectra for PCR/TiO_2/ITO, pDNA/TiO_2/ITO and TiO_2/ITO films.

These results contribute to better understanding the influence of the geometry of the different DNA molecules immobilized on nanostructured semiconductor and impact to the charge transfer processes in DNA molecules usually applied in electrochemical biosensors.

Acknowledgements

We would like to thank CNPq (573636/2008-7) (National Counsel of Technological and Scientific Development) and CAPES (15246.15) (Coordination for the Improvement of Higher Education Personnel) for financial support. Research partially supported by LNLS – Brazilian Synchrotron Light Laboratory, Brazil, through the research proposal SGM-16190.

Disclosure

The authors declare no competing financial interest.

Appendix A. Supplementary data

In Supporting information, we present the full sequence of bases of plasmid DNA and PCR. It is also shown the AFM image of TiO_2/ITO

substrate. Supplementary data to this article can be found online at https://doi.org/10.1016/j.saa.2018.03.081.

References

[1] P.J. Gomes, M. Coelho, M. Dionísio, P.A. Ribeiro, M. Raposo, Probing radiation damage by alternated current conductivity as a method to characterize electron hopping conduction in DNA molecules, Appl. Phys. Lett. 101 (2012) 123702–123706, https://doi.org/10.1063/1.4754287.

[2] L.G.D. Hawke, G. Kalosakas, C. Simserides, Electronic parameters for charge transfer along DNA, Eur. Phys. J. E. 32 (2010) 291–305, https://doi.org/10.1140/epje/i2010-10650-y.

[3] W.M. Hassen, C. Chaix, A. Abdelghani, F. Bessueille, D. Leonard, N. Jaffrezic-Renault, An impedimetric DNA sensor based on functionalized magnetic nanoparticles for HIV and HBV detection, Sensors Actuators B Chem. 134 (2008) 755–760, https://doi.org/10.1016/j.snb.2008.06.020.

[4] M.S. Hede, S. Fjelstrup, B.R. Knudsen, DNA sensors for malaria diagnosis, Nano Life 5 (2015) 1541003–1541012, https://doi.org/10.1142/S1793984415410032.

[5] C.Y. Yao, W.L. Fu, Biosensors for hepatitis B virus detection, World J. Gastroenterol. 20 (2014) 12485–12492, https://doi.org/10.3748/wjg.v20.i35.12485.

[6] P.R. Solanki, A. Kaushik, V.V. Agrawal, B.D. Malhotra, Nanostructured metal oxide-based biosensors, NPG Asia Mater. 3 (2011) 17–24, https://doi.org/10.1038/asiamat.2010.137.

[7] X. Zhang, F. Wang, B. Liu, E.Y. Kelly, M.R. Servos, J. Liu, Adsorption of DNA oligonucleotides by titanium dioxide nanoparticles, Langmuir 30 (2014) 839–845.

[8] M.A. Henderson, A surface science perspective on TiO_2 photocatalysis, Surf. Sci. Rep. 66 (2011) 185–297, https://doi.org/10.1016/j.surfrep.2011.01.001.

[9] C.L. Pang, R. Lindsay, G. Thornton, Chemical reactions on rutile TiO_2(110), Chem. Soc. Rev. 37 (2008) 2328–2353, https://doi.org/10.1039/b719085a.

[10] P.A. Connor, A.J. McQuillan, Phosphate adsorption onto TiO_2 from aqueous solutions: an in situ internal reflection infrared spectroscopic study, Langmuir 15 (1999) 2916–2921, https://doi.org/10.1021/la980894p.

[11] J. Liu, C. Roussel, G. Lagger, P. Tacchini, H.H. Girault, Antioxidant sensors based on DNA-modified electrodes, Anal. Chem. 77 (2005) 7687–7694, https://doi.org/10.1021/ac0509298.

[12] R.M. Green, J. Sambrook, Molecular Cloning - A Laboratory Manual, 4th ed. Cold Spring Harbor Press, New York, USA, 2012https://doi.org/10.3724/SP.J.1141.2012.01075.

[13] M.H. Habibi, M. Nasr-Esfahani, Preparation, characterization and photocatalytic activity of a novel nanostructure composite film derived from nanopowder TiO_2 and sol-gel process using organic dispersant, Dyes Pigments 75 (2007) 714–722, https://doi.org/10.1016/j.dyepig.2006.07.032.

[14] I. Horcas, R. Fernández, J.M. Gómez-Rodríguez, J. Colchero, J. Gómez-Herrero, A.M. Baro, WSXM: a software for scanning probe microscopy and a tool for nanotechnology, Rev. Sci. Instrum. 78 (2007)https://doi.org/10.1063/1.2432410.

[15] Y. Zubavichus, M. Zharnikov, A. Shaporenko, O. Fuchs, L. Weinhardt, C. Heske, E. Umbach, J.D. Denlinger, M. Grunze, Soft X-ray induced decomposition of phenylalanine and tyrosine: a comparative study, J. Phys. Chem. A 108 (2004) 4557–4565, https://doi.org/10.1021/jp049376f.

[16] C.D. Wagner, L.E. Davis, M.V. Zeller, J.A. Taylor, R.H. Raymond, L.H. Gale, Empirical atomic sensitivity factors for quantitative analysis by electron spectroscopy for chemical analysis, Surf. Interface Anal. 3 (1981) 211–225, https://doi.org/10.1002/sia.740030506.

[17] E. Farjami, L. Clima, K.V. Gothelf, E.E. Ferapontova, DNA interactions with a Methylene Blue redox indicator depend on the DNA length and are sequence specific, Analyst 135 (2010) 1443–1448, https://doi.org/10.1039/c0an00049c.

[18] S.O. Kelley, J.K. Barton, N.M. Jackson, M.G. Hill, Electrochemistry of Methylene Blue bound to a DNA-modified electrode, Bioconjugate 8 (1997) 31–37.

[19] C.G. Pheeney, J.K. Barton, DNA electrochemistry with tethered methylene blue, Langmuir 28 (2012) 7063–7070, https://doi.org/10.1021/la300566x.DNA.

[20] M.J. Dinsmore, J.S. Lee, Characteristic differences in the X-ray photoelectron spectrum between B-DNA and M-DNA monolayers on gold, J. Inorg. Biochem. 102 (2008) 1599–1606, https://doi.org/10.1016/j.jinorgbio.2008.02.007.

[21] P.J. Gomes, A.M. Ferraria, A.M. Botelho Do Rego, S.V. Hoffmann, P.A. Ribeiro, M. Raposo, Energy thresholds of DNA damage induced by UV radiation: an XPS study, J. Phys. Chem. B 119 (2015) 5404–5411, https://doi.org/10.1021/acs.jpcb.5b01439.

[22] M. Kulkarni, A. Mazare, J. Park, E. Gongadze, M.S. Killian, S. Kralj, K. von der Mark, A. Iglič, P. Schmuki, Protein interactions with layers of TiO_2 nanotube and nanopore arrays: morphology and surface charge influence, Acta Biomater. 45 (2016) 1–10, https://doi.org/10.1016/j.actbio.2016.08.050.

[23] R.A. Rosenberg, J.M. Symonds, K. Vijayalakshmi, D. Mishra, T.M. Orlando, R. Naaman, The relationship between interfacial bonding and radiation damage in adsorbed DNA, Phys. Chem. Chem. Phys. 16 (2014) 15319–15325, https://doi.org/10.1039/C4CP01649A.

[24] M.R. Vilar, A.M.B. Do Rego, A.M. Ferraria, Y. Jugnet, C. Noguès, D. Peled, R. Naaman, Interaction of self-assembled monolayers of DNA with electrons: HREELS and XPS studies, J. Phys. Chem. B 112 (2008) 6957–6964, https://doi.org/10.1021/jp8008207.

[25] C.X. Yan, R.G. Cavell, Gas phase phosphorus (1s and 2p) binding energy auger shifts in some polariable phosphorus compounds, J. Electron Spectros. Relat. Phenomena. 42 (1987) 49–60.

[26] T.C. Taucher, I. Hehn, O.T. Hofmann, M. Zharnikov, E. Zojer, Understanding chemical versus electrostatic shifts in X-ray photoelectron spectra of organic self-assembled monolayers, J. Phys. Chem. C 120 (2016) 3428–3437, https://doi.org/10.1021/acs.jpcc.5b12387.

[27] Z. Song, J. Hrbek, R. Osgood, Formation of TiO_2 nanoparticles by reactive-layer-assisted deposition and characterization by XPS and STM, Nano Lett. 5 (2005) 1327–1332, https://doi.org/10.1021/nl0505703.

[28] G. Iucci, C. Battocchio, M. Dettin, R. Gambaretto, C. Di Bello, F. Borgatti, V. Carravetta, S. Monti, G. Polzonetti, Peptides adsorption on TiO_2 and Au: molecular organization investigated by NEXAFS, XPS and IR, Surf. Sci. 601 (2007) 3843–3849, https://doi.org/10.1016/j.susc.2007.04.024.

[29] G. Iucci, C. Battocchio, M. Dettin, R. Gambaretto, G. Polzonetti, A NEXAFS and XPS study of the adsorption of self-assembling peptides on TiO_2: the influence of the side chains, Surf. Interface Anal. 40 (2008) 210–214, https://doi.org/10.1002/sia.2717.

[30] G. Iucci, M. Dettin, C. Battocchio, R. Gambaretto, C. Di Bello, G. Polzonetti, Novel immobilizations of an adhesion peptide on the TiO_2 surface: an XPS investigation, Mater. Sci. Eng. C 27 (2007) 1201–1206, https://doi.org/10.1016/j.msec.2006.09.038.

[31] A. Córdoba, M. Hierro-Oliva, M.Á. Pacha-Olivenza, M.C. Fernández-Calderón, J. Perelló, B. Isern, M.L. González-Martín, M. Monjo, J.M. Ramis, Direct covalent grafting of phytate to titanium surfaces through Ti—O—P bonding shows bone stimulating surface properties and decreased bacterial adhesion, ACS Appl. Mater. Interfaces 8 (2016) 11326–11335, https://doi.org/10.1021/acsami.6b02533.

[32] C. Viornery, Y. Chevolot, D. Léonard, B.O. Aronsson, P. Péchy, H.J. Mathieu, P. Descouts, M. Grätzel, Surface modification of titanium with phosphonic acid to improve bone bonding: characterization by XPS and ToF-SIMS, Langmuir 18 (2002) 2582–2589, https://doi.org/10.1021/la010908i.

[33] F. Liu, L. Lu, P. Xiao, H. He, L. Qiao, Y. Zhang, Effect of oxygen vacancies on photocatalytic efficiency of TiO_2 nanotubes aggregation, Bull. Kor. Chem. Soc. 33 (2012) 2255–2259, https://doi.org/10.5012/bkcs.2012.33.7.2255.

[34] X.-M. Xu, A. Ikai, Recovery and amplification of plasmid DNA with atomic force microscopy and the polymerase chain reaction, Anal. Chim. Acta 361 (1998) 1–7.

[35] T.S. Spisz, Y. Fang, I.N. Bankman, R.H. Reeves, J.H. Hoh, Automated DNA sizing by atomic force microscopy, Johns Hopkins APL Tech. Dig. 20 (1999) 135–142.

[36] G.R. Chagas, V.S.V. Satyanarayana, F. Kessler, G.K. Belmonte, K.E. Gonsalves, D.E. Weibel, Selective fragmentation of radiation-sensitive novel polymeric resist materials by inner-shell irradiation, ACS Appl. Mater. Interfaces 7 (2015) 16348–16356, https://doi.org/10.1021/acsami.5b03378.

[37] N.T. Samuel, C.Y. Lee, L.J. Gamble, D.A. Fischer, D.G. Castner, NEXAFS characterization of DNA components and molecular-orientation of surface-bound DNA oligomers, J. Electron Spectrosc. Relat. Phenom. 152 (2006) 134–142, https://doi.org/10.1016/j.elspec.2006.04.004.

[38] D.E. Weibel, F. Kessler, G.V. da S. Mota, Selective surface functionalization of polystyrene by inner-shell monochromatic irradiation and oxygen exposure, Polym. Chem. 1 (2010) 645–649, https://doi.org/10.1039/b9py00342h.

[39] V.S. Lusvardi, M.A. Barteau, J.G. Chen, J. Eng, B. Frühberger, A. Teplyakov, An NEXAFS investigation of the reduction and reoxidation of TiO_2(001), Surf. Sci. 397 (1998) 237–250, https://doi.org/10.1016/S0039-6028(97)00740-1.

[40] L. Soriano, M. Abbate, J. Vogel, J.C. Fuggle, A. Fernández, A.R. González-Elipe, M. Sacchi, J.M. Sanz, Chemical changes induced by sputtering in TiO_2 and some selected titanates as observed by X-ray absorption spectroscopy, Surf. Sci. 290 (1993) 427–435.

[41] F.R.R. Teles, L.P. Fonseca, Talanta trends in DNA biosensors, Talanta 77 (2008) 606–623, https://doi.org/10.1016/j.talanta.2008.07.024.

[42] R. Ruus, A. Kikas, A. Saar, A. Ausmees, E. Nõmmiste, J. Aarik, A. Aidla, T. Uustare, I. Martinson, Ti2p and O1s X-ray absorption of TiO_2 polymorphs, Solid State Commun. 104 (1997) 199–203, https://doi.org/10.1016/S0038-1098(97)00300-1.

[43] K.E. Lee, M.A. Gomez, T. Regier, Y. Hu, G.P. Demopoulos, Further understanding of the electronic interactions between N719 sensitizer and anatase TiO_2 films: a combined X-ray absorption and X-ray photoelectron spectroscopic study, J. Phys. Chem. C 115 (2011) 5692–5707.

[44] K.J.A. Raj, R. Shanmugam, R. Mahalakshmi, B. Viswanathan, XPS and IR spectral studies on the structure of phosphate and sulphate modified titania - a combined DFT and experimental study, Indian J. Chem. 49 (2010) 9–17.

[45] K. Syres, A. Thomas, F. Bondino, M. Malvestuto, M. Grätzel, Dopamine adsorption on anatase TiO_2(101): a photoemission and NEXAFS spectroscopy study, Langmuir 26 (2010) 14548–14555, https://doi.org/10.1021/la1016092.

[46] A.G. Thomas, M.J. Jackman, M. Wagstaffe, H. Radtke, K. Syres, J. Adell, A. Lévy, N. Martsinovich, Adsorption studies of p-aminobenzoic acid on the anatase TiO_2 (101) surface, Langmuir 30 (2014) 12306–12314, https://doi.org/10.1021/la5032619.